A comparative study of mass balance in the Lambert Glacier and Amery Ice Shelf along the Chinese inland traverse during 2019–2023 using altimetry, gravity, and in-situ observations

Hongwei Li [1, 2], Youquan He [1, 2], Yuanyuan Gu [1, 2], Gang Qiao [1, 2]

[1] Center for Spatial Information Science and Sustainable Development Applications, Tongji University, Shanghai 200092, China
[2] College of Surveying and Geo-informatics, Tongji University, Shanghai 200092, China - lihw@tongji.edu.cn; 1911211@tongji.edu.cn; 2111553@tongji.edu.cn; qiaogang@tongji.edu.cn

Keywords: ICESat-2, photon-counting laser altimetry, GRACE-FO, mass balance.

Abstract

The new photon-counting laser altimetry satellite ICESat-2 was successfully launched on September 15, 2018 with an unprecedented ice surface elevation measurement accuracy of 2-4 cm. It is meaningful for accurately estimating volumetric changes in the Antarctic Ice Sheet. Cross-validation of different types of data, especially comparison with in-situ data, is important for the ice sheet mass balance results of a new satellite. This paper proposes an elevation-difference method of grid elevation change rate model, based on ICESat-2 ATL11 elevation time series data, to distinguish the linear change trend of ice sheet surface elevation from the elevation change resulting from periodic precipitation. In order to compare the estimated elevation-change rate with the flux computed from in-situ snow stake velocity measurements and GRACE-FO gravity survey data, we made corrections for firn air content, elastic, and glacier isostatic adjustment. Based on the ATL11 data from 2019 to 2023, our results show that the ice sheet change in Basin 11 along the CHINARE traverse is from ~0.019 m yr^{-1} to ~0.121 m yr^{-1}, and the mass balance in the upstream of the traverse in Basin 11 is ~1.9±0.2 Gt yr^{-1}. It is comparable to ~2.4±1.2 Gt yr^{-1} from GRACE-FO during the same time period. Furthermore, the flux across traverse-11.9±1.1 Gt yr^{-1} is comparable to that of ~-9.7±0.9 Gt yr^{-1} across the same flux gate during 1997-2009 which is calculated based on GNSS-derived ice velocity observations, considering the time period difference and uncertainties.

1. Introduction

Ice surface elevation change is a fundamental parameter for quantifying the flux of ice mass discharged from the Antarctic Ice Sheet (AIS) into the Southern Ocean and its consequential impact on global sea level rise. Hence, the precise determination of these elevation changes is imperative for elucidating the AIS's response to climatic variations. Based on integrated analyses of gravimetric, altimetric, and optical and radar imaging satellite observations spanning from 1992 to 2020, the AIS exhibited a net mass loss of 2671±530 Gt. This negative mass balance predominantly arises from accelerated ice loss within the West Antarctica Ice Sheet (WAIS) at a rate of 82±9 Gt yr^{-1}, followed by the Antarctic Peninsula Ice Sheet (APIS) at 13±5 Gt yr^{-1}. In contrast, the East Antarctica Ice Sheet (EAIS) maintained a near-balanced state, with a mass loss of 3±15 Gt yr^{-1}. However, significant regional ice flow acceleration and mass loss have been observed in Wilkes Land within the EAIS since the 1960s. Furthermore, due to the extensive area of the EAIS, the uncertainty of mass balance based on altimetric observations may be enlarged. For instance, mass balance estimations of EAIS derived from ICESat (2003-2008) are inconsistent with the integrated analyses based on other mission results.

The new photon-counting laser altimetry satellite, Ice, Cloud, and Land Elevation Satellite-2 (ICESat-2), was successfully launched and has collected data since September 15, 2018 with an unprecedented ice surface elevation measurement accuracy of 2-4 cm (Markus et al., 2017). It is meaningful for accurately estimating volumetric changes in the Antarctic Ice Sheet and its associated contribution to global sea level rise (Neumann et al., 2019). Cross-validation of different types of data, especially comparison with in-situ data, is important for the ice sheet mass balance results of a new satellite. In this paper, based on ICESat-2 ATL11 elevation time series data, an elevation-difference method of grid elevation change rate is proposed to distinguish the linear change trend of ice sheet surface elevation from the elevation change caused by periodic precipitation.

Based on the proposed method, we estimated the latest mass balance (2019-2023) of Basin 11, and the results are compared with the gravity satellite (GRACE-FO) result and the in-situ observations along the section of the Chinese National Antarctic Research Expedition (CHINARE) traverse.

2. Study Area and Data

2.1 Study Area

This study focuses on regional ice-sheet changes (Basin 11) in the east part of the Lambert Glacier/Amery Ice Shelf system, which is the largest glacier/ice shelf system in East Antarctica. As shown in Figure 1, the blue line indicates the basin boundary (Zwally et al., 2015), the black line illustrates the grounding line (Rignot et al., 2011), and the red line illustrates the CHINARE traverse (Li et al., 2021).

The study area is located in the region of 69.9°S-76.3°S and 68.5°E-94.8°E, covering an area of ~252,857 km^2. The length of the CHINARE traverse is about 520km from Zhongshan Station to Taishan Station. The CHINARE traverses through the entire Basin 11. Along the CHINARE traverse, there have been a number of in-situ experiments performed for mass balance studies, including one for ICESat-2 mass balance accuracy validation.

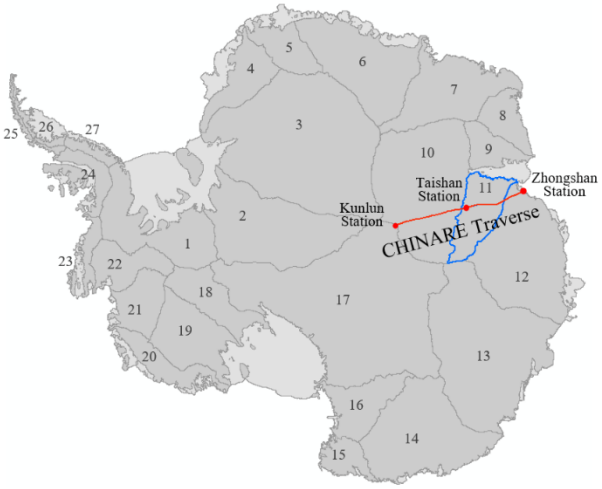

Figure 1. Study areas (red line and blue polygon) in AIS, Basin 11 along the CHINARE traverse.

2.2 Study Data

Multitype of data were used in the study, including ICESat-2 Annual Land Ice Height ATL11 data (https://nsidc.org/data/icesat-2/products), the High Spatial Resolution Mass Rates product from GRACE-FO (https://earth.gsfc.nasa.gov/geo/data/grace-mascons), in-situ measurements (Cui et al., 2020) along the CHINARE traverse, and the ERA5 wind speed product (https://cds.climate.copernicus.eu).

ATL11 is based on the ICESat-2 ATL06 Land Ice Height product, which provides height estimates for 40 m overlapping surface segments. ATL11 calculates elevations and elevation differences based on collections of segments from the same beam pair but from different cycles, with a spatial resolution of 60 m. It is intended as an input for high-level products (Ice Sheet Height Change ATL15 data), which will provide gridded estimates of ice-sheet height change, but also may be used alone, as a spatially-organized product that allows easy access to height-change information derived from ICESat-2. ATL11 employs a technique that builds upon those previously used to measure short-term elevation changes using ICESat repeat-track data. The ATL11 algorithm is similar to SERAC (surface elevation reconstruction and change detection), except that (1) polynomial fit correction is formulated somewhat differently, so that the ATL11 correction gives the surface height at the fit center, not the height residual, and (2) ATL11 does not include a polynomial fit with respect to time. ATL11 slope-corrected land ice height time series from cycle 3 to cycle 19 (Release 006) were used to calculate the ice surface elevation change rate of Basin 11 in this study.

GRACE-FO is the next-generation satellite of GRACE. GRACE and GRACE-FO gravimetry data are unique in their ability to observe global water mass variability and have frequently been applied for the determination of global mass rates to quantify the impacts of climate change and human activity on global freshwater availability and land ice evolution. Loomis et al. present a new global high-resolution mascon product that improves spatial resolution and signal recovery by estimating trends directly from more than 16 years of Level 1B GRACE and GRACE-FO data. High spatial resolution mass rates from GRACE-FO were used to estimate the mass balance of the ice sheet in the study area.

The in-situ measurements along the CHINARE traverse are from Cui et al. (2020). The traverse, which comprised airborne ice-penetrating radar survey lines, ice-flow monitoring stations at 30-km intervals, bamboo stakes (to measure snow accumulation) at 2-km intervals, and several automatic weather stations, had been established during several CHINARE. The whole traverse has since been studied in detail, including surface snow accumulation and ice-flow velocity. Cui et al. describe how to calculate the ice flux across the traverse using airborne observations of ice thickness and in situ measurements of ice flow velocity and surface snow accumulation.

In this paper, we discuss the mass balance of Basin 11 by comparing our ICESat-2 result with GRACE-FO and in-situ measurements.

3. Methods

3.1 Surface Elevation Change Detection

The analysis of ATL15 products shows that the surface elevation change rate dh/dt includes the seasonal change signal caused by periodic precipitation. It is not conducive to studying the long-term trend of the mass balance of the ice sheet. To distinguish the linear change trend of ice sheet surface elevation from the elevation change caused by periodic precipitation, we proposed an elevation-difference method of grid elevation change rate. It is divided into the following steps:

First, we remove error points according to the ATL11 quality label and set up the elevation-time equations by combining along-track and across-track elevation sequences (t_n, H_n).

$$\begin{cases} H_1 = \frac{dh}{dt}(t_1) + topography + seasonal(t_2) \\ H_2 = \frac{dh}{dt}(t_2) + topography + seasonal(t_2) \\ \cdots \\ H_n = \frac{dh}{dt}(t_n) + topography + seasonal(t_n) \end{cases} \quad (1)$$

where t_n, H_n = elevation H_n at time t_n on the ATL11 reference point

$topography$ = local topography

$seasonal$ = elevation change caused by periodic precipitation

$\frac{dh}{dt}$ = linear change trend of ice sheet surface elevation

Second, we make the elevation difference in pairs to remove the $topography$ term and convert elevation sequences (t_n, H_n) to elevation difference sequences $(\Delta H_{t_2-t_1}, t_1, t_2)$.

$$\Delta H_{t_2-t_1} = \frac{dh}{dt}(t_2 - t_1) + \left(\sum_{r=1}^{2}\left(d_r sin\left(\frac{2\pi t_2}{T_r}\right) + e_r cos\left(\frac{2\pi t_2}{T_r}\right) + f_r\right) - \sum_{r=1}^{2}\left(d_r sin\left(\frac{2\pi t_1}{T_r}\right) + e_r cos\left(\frac{2\pi t_1}{T_r}\right) + f_r\right)\right) \quad (2)$$

Based on the above transformation, we can combine the neighbouring ATL11 data together to solve surface elevation change rate dh/dt. There are C_n^2 combinations for each ATL11 point.

$$\begin{cases} \Delta H_{t_2-t_1} = F\left(t_1, t_2, \frac{dh}{dt}, d_1, e_1, T_1, d_2, e_2, T_2\right) \\ \Delta H_{t_3-t_1} = F\left(t_1, t_3, \frac{dh}{dt}, d_1, e_1, T_1, d_2, e_2, T_2\right) \\ \cdots \\ \Delta H_{t_j-t_i} = F\left(t_i, t_j, \frac{dh}{dt}, d_1, e_1, T_1, d_2, e_2, T_2\right) \end{cases} \quad (3)$$

where $\frac{dh}{dt}, d_1, e_1, T_1, d_2, e_2, T_2$ = fitting parameters of the curve. The seasonal cycle of the first order is generally considered to be one year, so T_1 is fixed to 365.

Then, we solve the equation iteratively based on least square method. The overfitting judgment is made based on the seasonal term obtained by the solution.
Last, based on 10 km girds, we calculate the mean and standard deviation of dh/dt, and exclude results beyond 3 times standard deviation.

3.2 Mass Balance Estimation

To validate the estimated elevation-change rate using the flux computed from in-situ snow stake velocity measurements and GRACE-FO gravity survey data, we make Firn Air Content (FAC), elastic, and Glacier Isostatic Adjustment (GIA) corrections for mass balance as follows:

$$\frac{dM}{dt} = \left(\frac{dV}{dt} - \frac{dFAC}{dt} - \frac{dEU}{dt} - \frac{dGIA}{dt}\right) \times \rho \quad (4)$$

where $\frac{dM}{dt}$ = mass balance
$\frac{dV}{dt}$ = ice sheet volume change
$\frac{dFAC}{dt}$ = FAC correction
$\frac{dEU}{dt}$ = GIA correction
$\frac{dGIA}{dt}$ = elastic correction
ρ = ice density

The volume change $\frac{dV}{dt}$ during the period can be computed through an integral of the change rates in the region where a Lambert azimuthal-equal area projection is used. $\frac{dFAC}{dt}$ is calculated based on the GSFC-FDM v1.2.1 (Figure 2a). $\frac{dEU}{dt}$ and $\frac{dGIA}{dt}$ come from Smith et al. (2020). The density distribution ρ of AIS used in the study was published by Hansen et al. (2023) (Figure 2b). Part of the details of ρ can be seen in the Appendix.

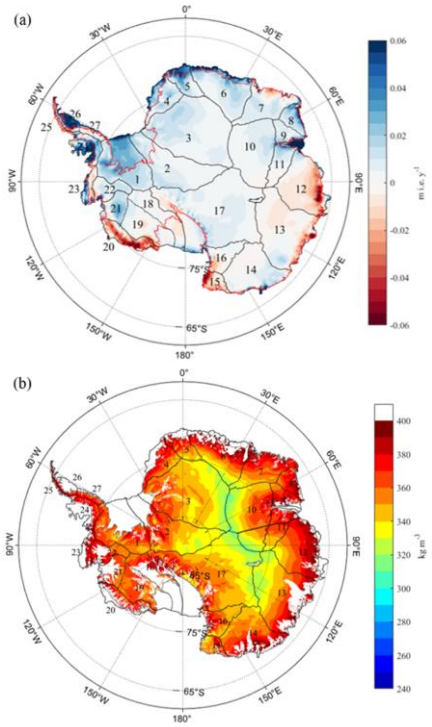

Figure 2. (a) $\frac{dFAC}{dt}$, and (b) ρ distribution in the AIS.

4. Results and Discussion

4.1 $\frac{dh}{dt}$ Fitting Results

To verify the reliability of our method, we randomly present the fitting results for four typical regions (Figure 3), which are relatively evenly distributed in the AIS, to examine the effectiveness of the precipitation term modelling on improving the elevation change rate estimation.

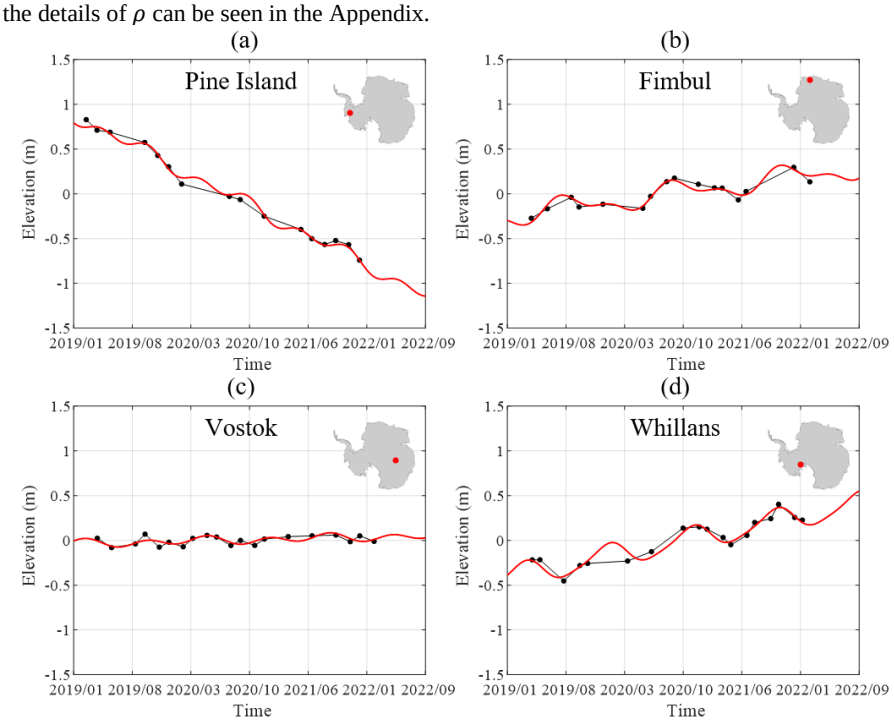

Figure 3. Fitting results for four typical regions (a) Pine Island, (b) Fimbul, (c) Vostok, and (d) Whillans.

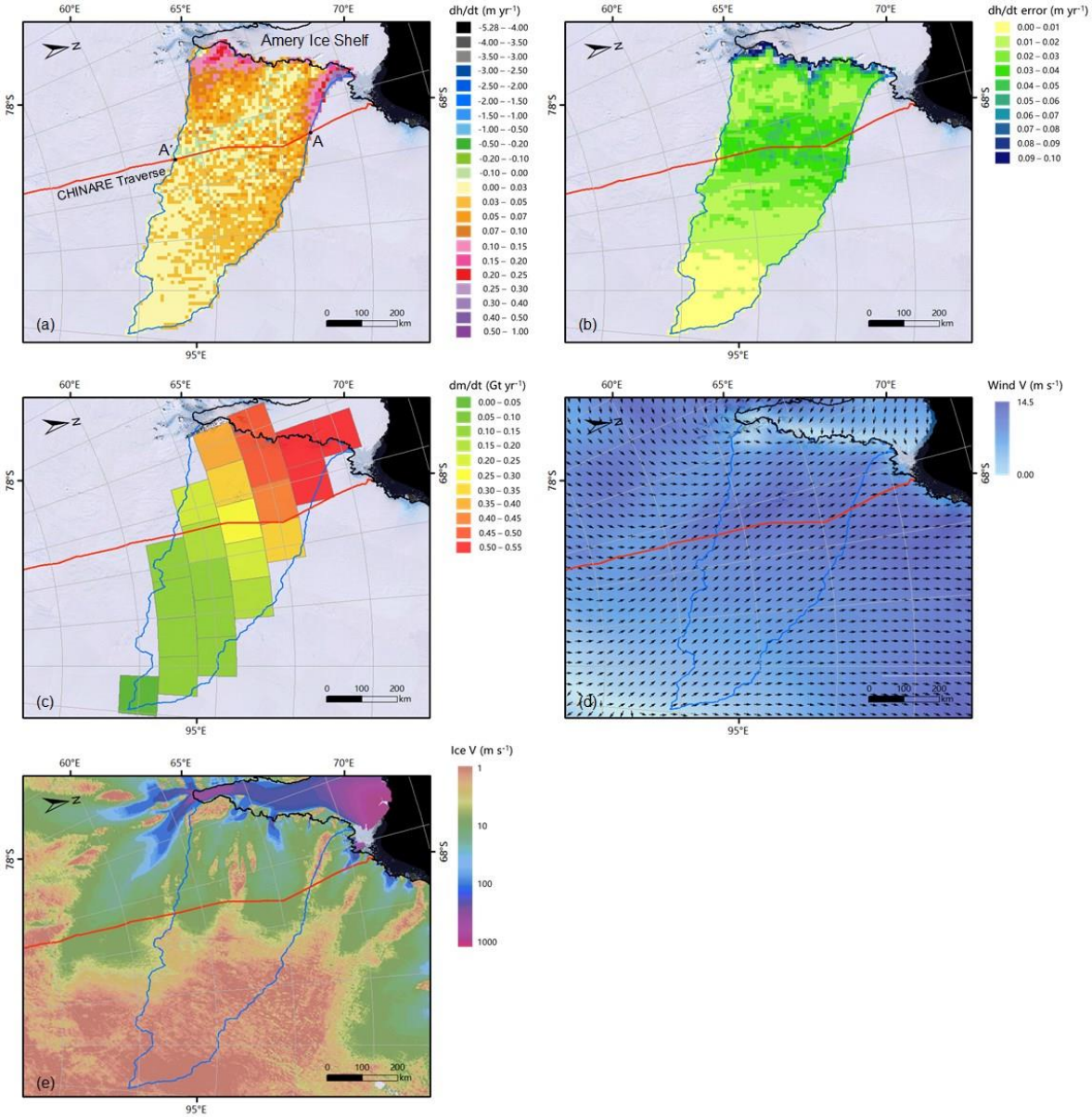

Figure 4. (a) Estimated ICESat-2 surface elevation change rate dh/dt in Basin 11. Grid spacing is 10 km. (b) Error of surface elevation change rate dh/dt in Basin 11. (c) Mass balance change rate dm/dt in Basin 11 based on GRACE-FO. (d) Average wind speed from ERA5 (2010-2020). Background is Landsat image mosaic of Antarctica (LIMA).

As shown in Figure 4, the periodical curves in all four points exhibit a seasonal cycle in the region that is represented by the fixed cycle of one year T_1 and adjusted locally by the unknown cycle T_2 separately.

Region	$\frac{dh}{dt}$ (m yr^{-1})	Curve fitting error (m)
Pine Island	-0.475	0.108
Fimbul	0.224	0.025
Vostok	0.016	0.013
Whillans	0.197	0.024

Table 1. Elevation change rates, uncertainty and periodical curve fitting error in four typical regions.

As shown in Figure 4 and Table 1, the results show that our method has a good fitting effect for both the ablation area (Pine Island), accumulation area (Fimbul, Whillans), as well as the area with a small surface elevation change (Vostok). Except for Pine Island, the resulting curve fitting error ranges from ~1.3 to ~2.5 cm. Relative to the elevation change rate of -0.475 m yr^{-1}, the curve fitting error of 0.108 m is also acceptable.

Using ICESat-2 ATL11 data from 2019 to 2023, our $\frac{dh}{dt}$ results show that the ice sheet change in Basin 11 along the Chinese inland traverse is from ~0.019 m yr^{-1} to ~0.121 m yr^{-1} (Figure 4a). The elevation change rate estimated in Basin 11 shows an overall thickening in this eastern tributary region of the Amery Ice Shelf, with an average rate of ~0.046 m yr^{-1}. The average uncertainty of dh/dt is ~0.026 m yr^{-1} (Figure 4b). The uncertainty in the inland flat area of the ice sheet is small (0.01-0.03 m yr^{-1}), and the uncertainty near the ground line is large (0.07-0.09 m yr^{-1}). Along

the section of the CHINARE traverse that cuts through the basin, the average rate is relatively low, at ~0.040 m yr^{-1}.
There is a west-ward increasing trend of thickening from the inland interior to the Amery Ice Shelf. The overall low rate and the increasing trend in this region coincide with its descending terrain and katabatic wind (Figure 4d) effect, which transports surface now from this side of the ice shelf to the other side (Scambos et al., 2012; Ding et al., 2011; Fricker et al., 2000).

4.2 Comparison and Discussion of Mass Balance (Basin 11)

In this study, the elevation change rate obtained based on ICESat-2 is compared with the in-situ measurements along the CHINARE traverse. Surface height change that is mainly attributed to snow accumulation is measured by using snow stakes. The cross section within Basin 11 (AA’ in Figure 4a) contains 192 stakes spaced approximately 2 km apart. The 30 km moving window was used for average filtering, and the data was smoothed (thick red line in Figure 5). The average dynamic elevation change rate is 0.199 m/y, which is the difference between the average surface height change rate (0.239 m yr^{-1}, red dotted line in Figure 5) and the average surface elevation change rate (0.040 m yr^{-1}, blue dotted line in Figure 5). According to the distribution of the average dynamic elevation change rate of the traverse, the average dynamic elevation change rate of the area near the coastline is larger than that in the inland area.

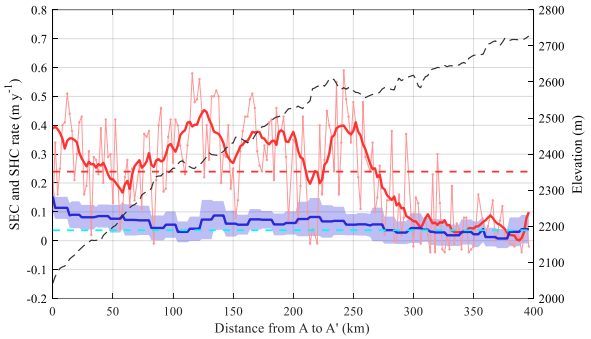

Figure 5. Data used for flux calculation across profile AA’ in Basin 11 along the CHINARE traverse: ICESat-2 surface elevation change rate from 2019 to 2023 (blue line) and stake surface height change rate from 2019-2023 (thick red line) which is smoothed from the original stake measurements (thin red line). Dashed blue and red lines are their respective averages. Dashed black line shows elevations along the profile.

Then surface elevation changes in all grid cells in the upstream region of AA’ section are counted to obtain the total snow volume change rate. Based on the ice and snow surface density distribution ρ, the volume change rate is converted into the overall mass balance of the upstream region of the AA’ section (~1.9±0.2 Gt yr^{-1}). Thus, by subtracting the mean surface mass balance (13.8±0.1 Gt yr^{-1}) from the total mass balance above, the ice flux across traverse AA’ -11.9±1.1 Gt yr^{-1} is comparable to that of ~-9.7±0.9 Gt yr^{-1} across the same flux gate during 1997-2009 that is calculated based on GNSS-derived ice velocity observations (Cui et al., 2020), considering the time period difference and uncertainties.
Loomis et al. (2021) presented a new global high-resolution mascon product that improves spatial resolution and signal recovery by estimating trends directly from GRACE-FO data. Based on this gravity mass balance product, we estimate the mass balance change rate of Basin 11 (Figure 4c). The mass balance in the region upstream of the traverse in Basin 11 is calculated as ~1.9±0.2 Gt yr^{-1} from ICESat, which is comparable to ~2.4±1.2 Gt yr^{-1} from GRACE-FO during the same time period. Although the gravity results have a lower spatial resolution, there is a similar west-ward increasing trend of thickening from the inland interior to the Amery Ice Shelf (Figure 4c).
In general, the experimental results show that the mass balance results of ICESat-2 in Basin 11 have a high agreement level of with the gravity results and the in-situ measured results. Due to the large variation among different basins, more observational data are needed to verify and evaluate the latest ICESat-2 mass balance results for AIS.

Acknowledgements

This work was supported by the National Key Research and Development Program of China (no. 2021YFB3900105, 2022YFC2807105), the National Natural Science Foundation of China (grant no. 42276249, 42394131, 42111530185), and Fundamental Research Funds for the Central Universities.
We also thank the NASA National Snow and Ice Data Center (NSIDC) for supplying the ICESat-2 data and GSFC for GSFC-FDM v1.2.1.

References

Markus, T., Neumann, T., Martino, A., Abdalati, W., Brunt, K., Csatho, B., ... & Zwally, J., 2017: The Ice, Cloud, and land Elevation Satellite-2 (ICESat-2): science requirements, concept, and implementation. *Remote sensing of environment*, 190, 260-273.

Neumann, T. A., Martino, A. J., Markus, T., Bae, S., Bock, M. R., Brenner, A. C., ... & Thomas, T. C., 2019: The Ice, Cloud, and Land Elevation Satellite–2 Mission: A global geolocated photon product derived from the advanced topographic laser altimeter system. *Remote sensing of environment*, 233, 111325.

Zwally, H. J., Li, J., Robbins, J. W., Saba, J. L., Yi, D., & Brenner, A. C., 2015: Mass gains of the Antarctic ice sheet exceed losses. *Journal of Glaciology*, 61(230), 1019-1036.

Li, R., Li, H., Hao, T., Qiao, G., Cui, H., He, Y., ... & Li, B., 2021: Assessment of ICESat-2 ice surface elevations over the Chinese Antarctic Research Expedition (CHINARE) route, East Antarctica, based on coordinated multi-sensor observations. *The Cryosphere*, 15(7), 3083-3099.

Cui, X., Du, W., Xie, H., & Sun, B., 2020: The ice flux to the Lambert Glacier and Amery Ice Shelf along the Chinese inland traverse and implications for mass balance of the drainage basins, East Antarctica. *Polar Research*.

Smith, B., Fricker, H. A., Holschuh, N., Gardner, A. S., Adusumilli, S., Brunt, K. M., ... & Siegfried, M. R., 2019: Land ice height-retrieval algorithm for NASA's ICESat-2 photon-counting laser altimeter. *Remote Sensing of Environment*, 233, 111352.

Scambos, T. A., Frezzotti, M., Haran, T., Bohlander, J., Lenaerts, J. T. M., Van Den Broeke, M. R., ... & Winther, J. G., 2012: Extent of low-accumulation'wind glaze'areas on the East Antarctic plateau: implications for continental ice mass balance. *Journal of glaciology*, 58(210), 633-647.

Minghu, D., Cunde, X., Yuansheng, L., Jiawen, R., Shugui, H., Bo, J., & Bo, S., 2011: Spatial variability of surface mass balance

along a traverse route from Zhongshan station to Dome A, Antarctica. *Journal of Glaciology*, 57(204), 658-666.

Fricker, H. A., Warner, R. C., & Allison, I., 2000: Mass balance of the Lambert Glacier–Amery Ice Shelf system, East Antarctica: a comparison of computed balance fluxes and measured fluxes. *Journal of Glaciology*, 46(155), 561-570.

Appendix

Hansen et al. (2023) considered horizontal ice velocity, surface elevation change rate, and equilibrium line altitude (ELA) to determine the latest Antarctic ice density parameters based on the following criteria:

Below ELA, the surface density ρ is assumed to be the density of ice (917 kg m^{-3}), i.e., all snow melts during the melt season.

In the region above ELA, where the horizontal ice velocity is greater than 30 m y^{-1} and $\frac{dh}{dt}$ is negative, assuming that the change in ice elevation is caused by ice dynamics, the value ρ = 917 kg m^{-3} is assigned. Here, the selection of the horizontal ice velocity threshold is based on the work of Nilsson et al. (2022).

In regions where $\frac{dh}{dt}$ is positive and dynamic ice accumulation is known, ρ = 917 kg m^{-3} is also used (Basin 11 has no such area).

For other places, the density of the snow used is estimated by the model (250-400 kg m^{-3}).